

University of Groningen

Elucidation of mechanisms in manganese and iron based oxidation catalysis

Angelone, Davide

IMPORTANT NOTE: You are advised to consult the publisher's version (publisher's PDF) if you wish to cite from it. Please check the document version below.

Document Version

Publisher's PDF, also known as Version of record

Publication date:

2016

[Link to publication in University of Groningen/UMCG research database](#)

Citation for published version (APA):

Angelone, D. (2016). *Elucidation of mechanisms in manganese and iron based oxidation catalysis: Mechanistic insights and development of novel approaches applied to transition metal catalyzed oxidations catalysis*. [Thesis fully internal (DIV), University of Groningen]. University of Groningen.

Copyright

Other than for strictly personal use, it is not permitted to download or to forward/distribute the text or part of it without the consent of the author(s) and/or copyright holder(s), unless the work is under an open content license (like Creative Commons).

The publication may also be distributed here under the terms of Article 25fa of the Dutch Copyright Act, indicated by the "Taverne" license. More information can be found on the University of Groningen website: <https://www.rug.nl/library/open-access/self-archiving-pure/taverne-amendment>.

Take-down policy

If you believe that this document breaches copyright please contact us providing details, and we will remove access to the work immediately and investigate your claim.

Downloaded from the University of Groningen/UMCG research database (Pure): <http://www.rug.nl/research/portal>. For technical reasons the number of authors shown on this cover page is limited to 10 maximum.

Chapter 5

Elucidation of the mechanism of manganese catalysed oxidation of alkenes in aqueous media at high pH

The oxidation of substrates, such as water soluble alkenes, with H_2O_2 with the catalyst $[\text{Mn(IV,IV)}_2(\mu\text{-O})_3(\text{tmtacn})_2]^{2+}$ (**1**) is studied in this chapter with the goal of elucidating the role of both 'free' Mn(II) ions and carbonate as a buffer. The chapter focuses on the effect of buffers, concentration and sequestrant on catalytic activity. The main finding is that mechanistic studies must recognize the possibility of concurrent catalytic processes being involved and consideration of the effect this has on results gained with variation in conditions and with probes is shown to be essential.

5.1 Introduction

The selective oxidation of organic compounds is as central to synthetic chemistry as to industrial chemical processes.^[1,2] Terminal oxidants of choice are O₂ and H₂O₂, primarily due to the minimal chemical impact they and their by-products have on the environment and above all their atom and economic efficiency. The direct use of O₂ and H₂O₂, although thermodynamically favourable is kinetically impeded and hence catalysts are central to their application. Over recent decades, intensive efforts have been directed toward the discovery and development of transition metal based catalysts for the activation of H₂O₂, not least for dihydroxylation and/or epoxidation of olefins and oxidation of other functional groups.^[3] Among the many first row transition metal catalysts reported to date, manganese complexes bearing ligands based on the ligand 1,4,7-trimethyl-1,4,7-triazacyclononane (tmtacn) such as **1** (Figure 1) have attracted considerable attention both for their solid state and magnetic properties and as models for bioinorganic systems.^[4] In the mid-1990s, the catalytic activity of the complex [Mn₂^{IV,IV}(μ-O)₃(tmtacn)₂](PF₆)₂ (**1**) was discovered in oxidation and bleaching process by Hage et al.^[4b] The application of manganese complexes of tacn in a wide range of oxidative functional group transformations in organic solvents was reviewed recently by Saisaha et al.^[5] and by Watkinson et al.^[6]

Although the solid state and magnetic properties of these complexes have been examined in detail,^[4a] the speciation of these complexes in solution and especially in water has received much less attention.^[7] Recent mechanistic studies into manganese catalyzed oxidation catalysis in particular speciation analysis in non-aqueous media, have shown the key role of the formation of μ-carboxylato bridged ([Mn(III,III)₂(μ-O)(μ-RCO₂)₂(tmtacn)₂]²⁺) complexes (e.g., **2**) formation in the case of **1**, which determines activity and selectivity in the oxidation of alkenes.^[8] It was proposed based on ESI-MS experiments and ¹⁸O-labeling studies that the dinuclear bis(carboxylato) bridged Mn(III,III)₂(OH)(OOH) species is a key intermediate in the formation of epoxide or *cis*-diol products.^[8] In chapter 4, the conversion of **1** to [Mn(III,III)₂(μ-O)(μ-RCO₂)₂(tmtacn)₂]²⁺ was studied in detail using a combination of UV/Vis absorption, electron paramagnetic resonance (EPR), Raman and resonance Raman (rR) spectroscopy. We proposed that the conversion proceeds by an autocatalytic mechanism and that the species that is responsible for the oxidation of the organic substrates also catalyzes H₂O₂ decomposition, and the former process is competitive.^[9] The ability of manganese catalysts to activate H₂O₂ to oxidize various azo and phenolic dyes in aqueous carbonate buffers was studied by Eldik and co-workers.^[10] The formation of a Mn(II) -HCO₃ complex was proposed on the basis of UV/Vis absorption spectroscopy and electrochemistry. Precipitation of Mn(II)CO₃ was observed in the absence of substrates, while addition of the azo and polyphenolic dyes inhibited the precipitation through complexation. The formation of the catalytically inactive species (Mn(IV)O₂) upon reaction of Mn(II) with H₂O₂ in NaHCO₃(aq) was confirmed by UV/Vis absorption spectroscopy and ESR.^[11] Kinetic analysis was interpreted as indicating that peroxycarbonate, a more reactive oxidant than H₂O₂, formed in situ and presented the rate-limiting step in the reaction.^[12] Comparison of the catalytic activity of Mn(II) salts with [Mn(II)(bpy)₂Cl₂] and [Mn(III)Mn(IV)(μ-O)₂(bpy)₄](ClO₄)₃·2H₂O in the bleaching of dyes indicated common reactive intermediates.

In this chapter the focus is on understanding the behavior of complexes such as **1** during catalytic oxidations under conditions relevant to modern industrial bleaching. The activity of the catalytic system (i.e. **1**) in the oxidation of styrene sulfonate, a conjugated olefin with high solubility in aqueous media, is studied, due primarily to its lack of pH chemistry (Figure 1). The pH dependence of the structure of the complex present in water between pH 6 and 9; the rate of oxidation of styrene with **1** and with Mn(II) salts; and the role of sequestrants, such as DTPA, that are used industrially, on the reaction rate and efficiency were studied with UV/Vis absorption and Raman spectroscopy. The study of the reactivity of Mn(II) under the same conditions was carried out to exclude or implicate the species it forms, in the chemistry observed with **1**; i.e. is **1** a catalyst or simply a source of Mn(II). Here, the major part is focused on control experiments with Mn(II) salts and the effect of variation in the amount of carbonate.

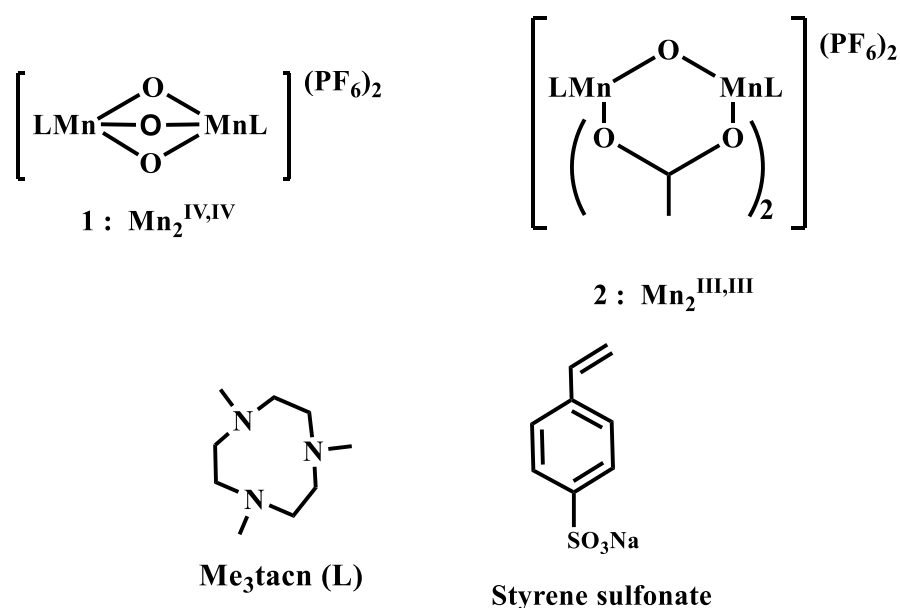
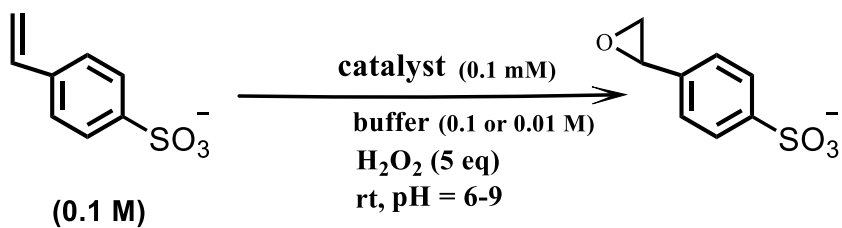
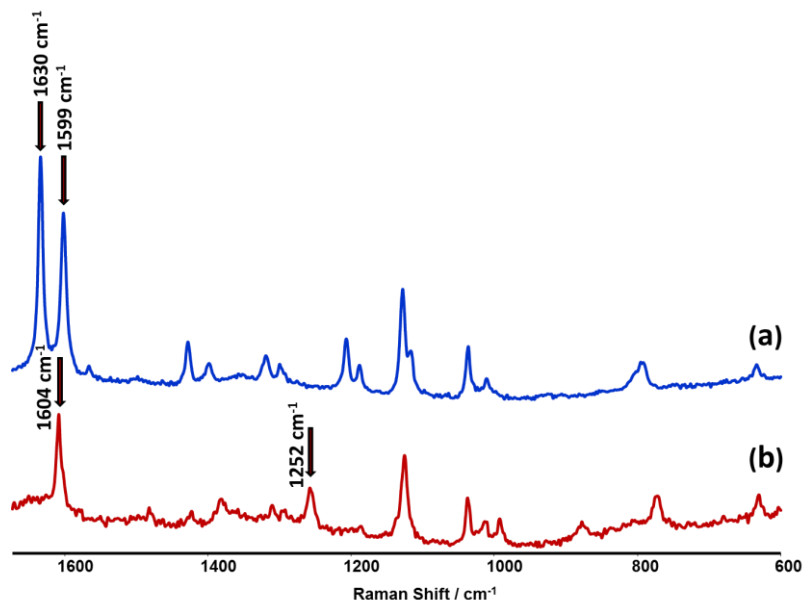


Figure 1 Structure of complexes **1** and **2**, the ligand tmtacn and substrates styrene sulfonate (SS)

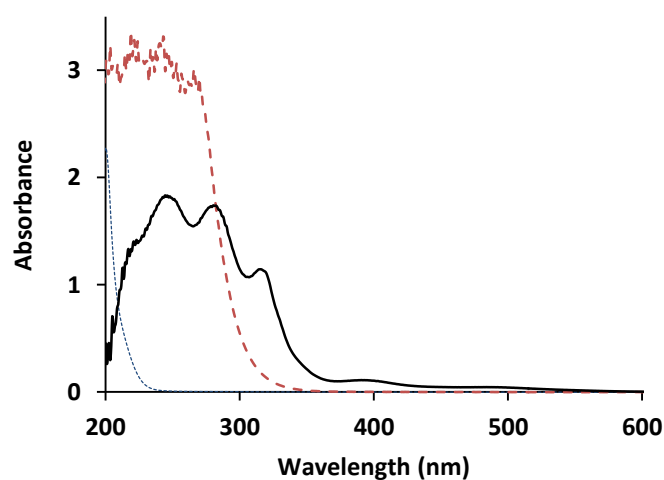
5.2 Results

Reaction monitoring by UV/Vis absorption, Raman and resonance Raman spectroscopy

Scheme 1 shows typical reaction conditions applied in the present study. The activity of **1** and Mn(II) ions was investigated and compared in the absence and presence of bicarbonate, acetate and borate (common reagents employed in industrial bleaching processes). Raman spectroscopy was used to monitor changes in the concentration of styrene sulfonate and its epoxide product. The bands in the range $1600\text{--}1650\text{ cm}^{-1}$ are characteristic of C=C stretching vibrations of vinyl and aryl groups and in particular the band at 1630 cm^{-1} is useful in monitoring reaction progress.^[13]

Scheme 1 Catalysed oxidation of styrene sulfonate (SS) with H₂O₂.Figure 2 Raman spectra (λ_{exc} 785 nm) of (a) SS and (b) the epoxide product OSS

The UV/Vis absorption spectra of **1**, H₂O₂ and 0.1 M carbonate buffer (w.r.t. water) are shown in Figure 3. Despite the complete absorption of light by H₂O₂ in the UV region, the visible absorption bands of **1** enable monitoring of its concentration and changes to the complex over time, e.g., by monitoring absorbance at 315 nm.

Figure 3 UV/Vis absorption spectra of **1** (0.1 mM, thick line), H₂O₂ (0.5 M, dashed line) and bicarbonate (0.1 M, dotted line) with respect to water as reference.

Stability of **1** in carbonate buffer in the presence of H_2O_2

The effect of the bicarbonate/carbonate on the structure of **1** was monitored by Raman spectroscopy (λ_{exc} 355 nm, Figure 4) over 23 h after the addition of H_2O_2 . The spectrum after 23 h shows the complete consumption of the H_2O_2 (876 cm^{-1}) without significant disturbance of the $\text{Mn}(\mu\text{-O}_3)\text{Mn}$ core of **1** (699 cm^{-1}).

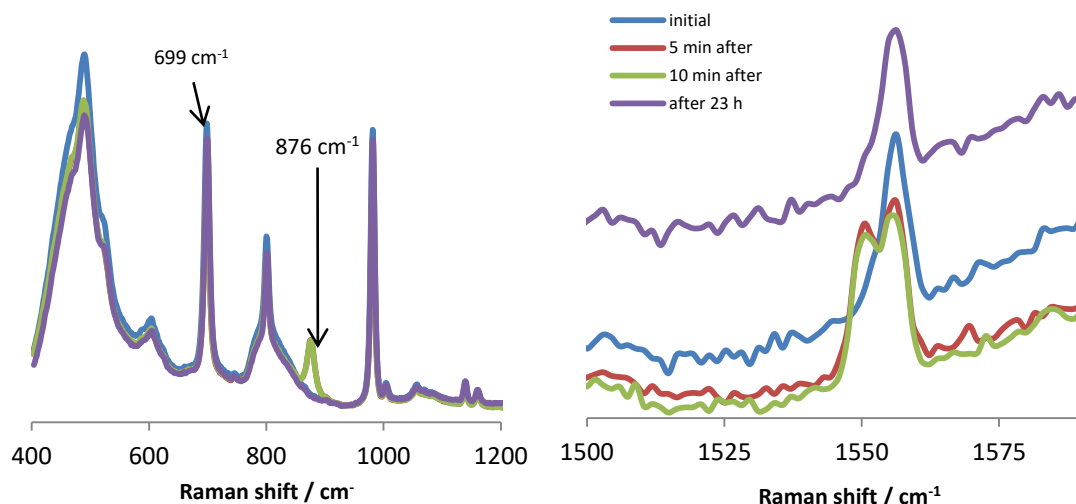


Figure 4 Raman spectra (λ_{exc} 355 nm) of a solution of H_2O_2 (0.5 M), and **1** (3 mM) in NaHCO_3 (aq. 0.1 M, pH 8.6) (left) and increase in dissolved O_2 (1550 cm^{-1}) (right). Spectra acquired before (blue), and 5 min (red), 10 min (green) and 23 h (purple) after the addition of H_2O_2 .

It is apparent that in $\text{NaHCO}_3(\text{aq})$, H_2O_2 has no noticeable effect on **1** manifested in the constancy of the Raman band of **1** at 699 cm^{-1} and absorption spectrum^[9,14] but that H_2O_2 decomposition proceeds quickly through disproportionation to water and O_2 (1550 cm^{-1}).

Dependence of the rate of oxidation of styrene sulfonate on the concentration of **1** and of Mn(II)SO_4

The rate of epoxidation of styrene sulfonate and the disproportionation of H_2O_2 in $\text{NaHCO}_3(\text{aq})$ (0.4 M, pH 8.6) was determined with **1** over the concentration range 50 – 200 μM and with Mn(II)SO_4 between 0 – 200 μM (Figure 5). The rate of epoxidation of styrene sulfonate shows a linear dependence on the concentration of **1**, however, the rate of disproportion of H_2O_2 , shows no dependence. Notably, however, the duration of the lag period before which H_2O_2 disproportionation commenced was inversely dependent on the concentration of **1**. In contrast to **1**, with $\text{Mn(II)(SO}_4)$ both the rate of epoxidation of styrene sulfonate as well as the disproportion of H_2O_2 depend logarithmically on concentration.

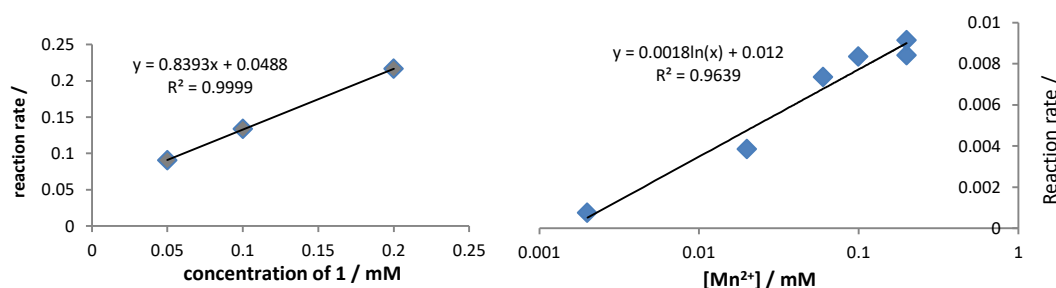


Figure 5 Dependence of the rate of the oxidation of the styrene sulfonate (right) on **1** and (left) on $\text{Mn(II)(SO}_4)$.

The logarithmic trend in both the rate of disproportionation and styrene sulfonate oxidation indicates that the actual concentration of 'available' manganese ions in the presence of carbonate is limited both by solubility and by the rate of formation of insoluble manganese oxides – indeed examination of the Pourbaix plot for manganese indicates that Mn(II) is not stable at pH 8.6. Indeed in the absence of styrene sulfonate a dark precipitate formed rapidly upon addition of H_2O_2 to a bicarbonate buffered solution of Mn(II)SO_4 . The Raman spectrum of the precipitate (Figure 6) obtained after the reaction of Mn(II) ions with H_2O_2 in the absence or presence of substrate show differences when compared to the spectrum of MnCO_3 , in particular the bands at $\sim 580\text{ cm}^{-1}$ and $\sim 630\text{ cm}^{-1}$, which are characteristic of Mn oxides.^[15,16]

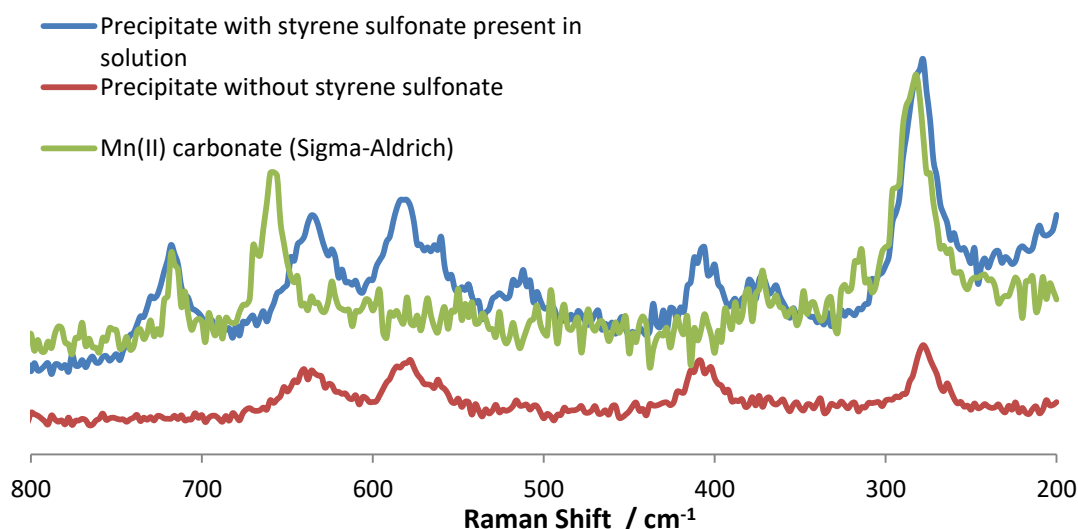


Figure 6 Raman spectrum of MnCO_3 (green line) and the spectrum of the precipitate obtained after addition of H_2O_2 to the solution containing MnSO_4 (0.2 mM) and NaHCO_3 (0.1 M) (red line) and with SS (blue line).

Cooperative effects between **1** and Mn(II)

The oxidation of styrene sulfonate and the disproportionation of H_2O_2 in presence of both **1** and Mn(II) was considered, since **1** could be acting simply as a 'slow leak' source of Mn(II). The reaction was carried out with continuous variation of **1** and Mn(II)SO_4 , with a constant concentration of 0.2 mM in manganese. Remarkably the effect of variation on both the rate of H_2O_2 disproportionation and styrene sulfonate oxidation is negligible, which indicates that under these conditions, the same catalytically active species (i.e. not **1** or its derivatives) is responsible primarily.

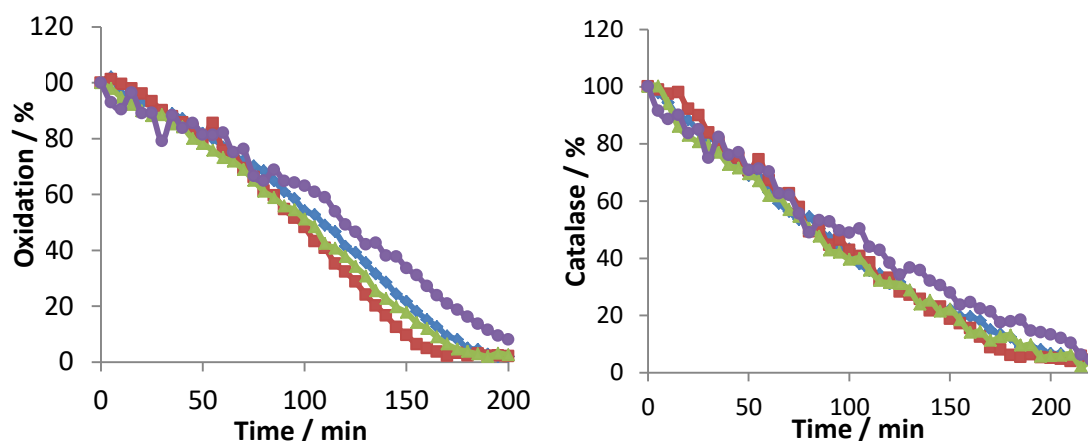


Figure 7 Oxidation of styrene sulfonate with H_2O_2 in the presence of various mole ratios of **1** and $\text{Mn(II)(SO}_4\text{)}$. Monitor by Raman spectroscopy at λ_{exc} 785 nm. Left: % styrene sulfonate remaining and Right: % H_2O_2 remaining. Reaction conditions: sodium sulfate (0.5 M) as internal reference, H_2O_2 (0.5 M), NaHCO_3 (0.1 M), styrene sulfonate (0.1 M), and MnSO_4 and **1** in ratios $\text{Mn(II)} / (\text{Mn(IV)} + \text{Mn(II)})$: 0 (blue diamonds); 0.5 (red squares); 0.3 (green triangles); 1 (purple circles).

Effect of DTPA on the catalytic oxidation of styrene sulfonate with **1** or Mn(II)SO_4

A frequently used approach to eliminate the effect of adventitious metal ions in aqueous reactions is to add a sequestrant, which by virtue of its multidenticity prevents the metal ion from engaging in catalysis. Hence, the activity of Mn(II)SO_4 is expected to be eliminated upon addition of the sequestrant DTPA (Penta(carboxymethyl)diethylenetriamine). The effect of DTPA on the oxidation of styrene sulfonate with H_2O_2 in the presence of **1** was determined with in situ reaction monitoring by Raman spectroscopy. With Mn(II)SO_4 , conversion was not observed in the presence of DTPA, while with **1**, activity was observed albeit with the addition of a lag phase that affected the oxidation of styrene sulfonate more so than H_2O_2 . These data indicate that although DTPA inhibits the reaction catalysed by Mn(II)SO_4 , it has a lesser effect on the activity of **1**. An experiment that raises a question mark over this conclusion is illustrated Figure 9.

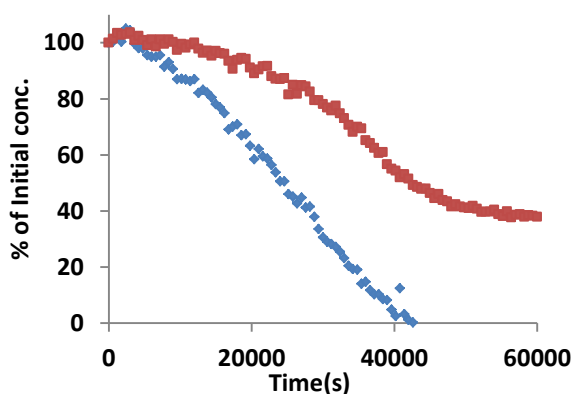


Figure 8 Change in concentration of H_2O_2 (0.5 M) and styrene sulfonate (0.1 M), in NaHCO_3 (aq., 0.4 M, pH 8.6), with **1** (0.1 mM), and DTPA (0.1 mM). Conversion was determined from the normalised intensity of Raman bands due to H_2O_2 (876 cm^{-1} , blue diamond's) and styrene sulfonate (1633 cm^{-1} , red squares).

Comparison of the reaction progress without DTPA present with an equivalent reaction in which DTPA is added after 50% conversion (Figure 9), shows that, even with **1**, DTPA does in fact stop conversion. Notably, however, after a considerable period of time, conversion continues again

with a rate similar to that observed without DTPA. These data indicated that a sudden change occurred in the reaction conditions.

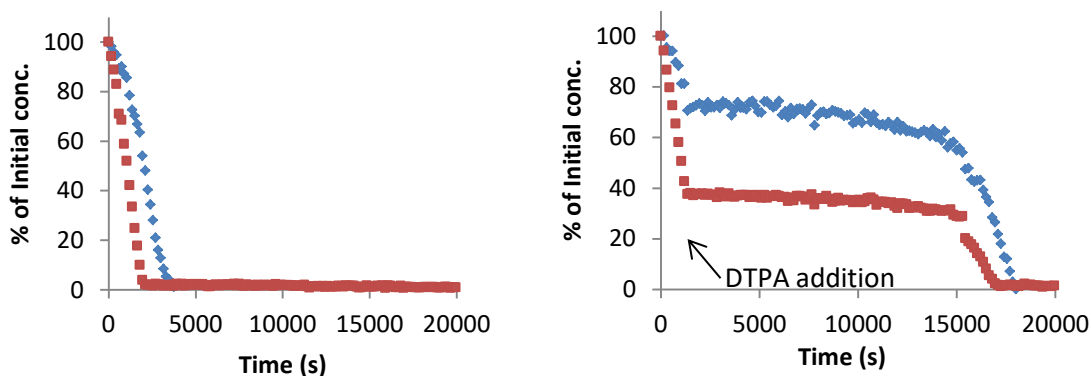


Figure 9 Oxidation of styrene sulfonate (0.1 M) with H₂O₂ (0.5 M) catalysed by **1**, and Na₂SO₄ (0.5 M) at pH 8.6 (0.2 M NaHCO₃). Styrene sulfonate (1633 cm⁻¹, red squares) and H₂O₂ (876 cm⁻¹, blue diamonds) were monitored by Raman spectroscopy. (left) Without DTPA, and (right) with DTPA (0.1 mM) added after 1350 s.

Addition of H₂O₂ to a solution of **1** in 0.1 M NaHCO₃(aq) has no effect on the latter's absorption spectrum between pH 6 and 9 even over several hours in the absence of substrate. Furthermore, there is no evidence for significant decomposition of H₂O₂ over this period. The UV/Vis absorption spectrum of the reaction mixture (i.e. the absorbance of **1**) does not change significantly over the entire course of the reaction under standard conditions also (Figure 10). Reaction of **1** with H₂O₂ in the presence of 1 eq. of DTPA, however, shows a pH dependent lag phase after which a large change in the UV/Vis absorption spectrum is observed indicative of conversion of **1** to another species (Figure 10). A reasonable interpretation of the data is that an autocatalytic reaction leading to decomposition of the DTPA occurs rapidly at the end of the lag period, which 'unlocks' the reaction to Mn(II) salts formed by reduction of **1**.

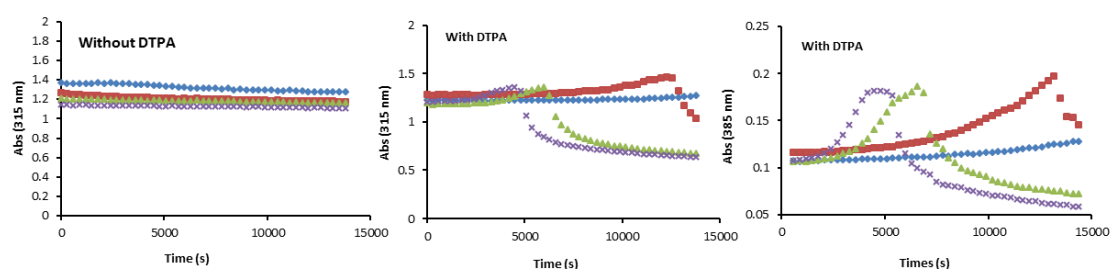


Figure 10 pH dependence of the change in absorbance of the reaction mixture (without styrene sulfonate) at 315 nm with 0.5 M H₂O₂, 0.1 M bicarbonate, 0.1 mM **1** (left) and with 0.1 mM DTPA also (centre and right). pH 8.9 (purple crosses), 8.0 (green triangles), 7.2 (red squares), 6.1 (blue diamonds).

Effect of buffering agents on the reaction rate

The rate of epoxidation of styrene sulfonate in the presence of borate, acetate, water and bicarbonate was determined by reaction monitoring with Raman spectroscopy (λ_{ex} 785 nm). As described above conversion under standard conditions is rapid in 0.1 M NaHCO₃(aq), whereas conversion is substantially slower without buffer or with acetate buffer and in borate buffer

conversion is not observed (Figure 11). These data raise the question whether carbonate is essential to the reactivity observed or if the other buffers inhibit the reactivity.

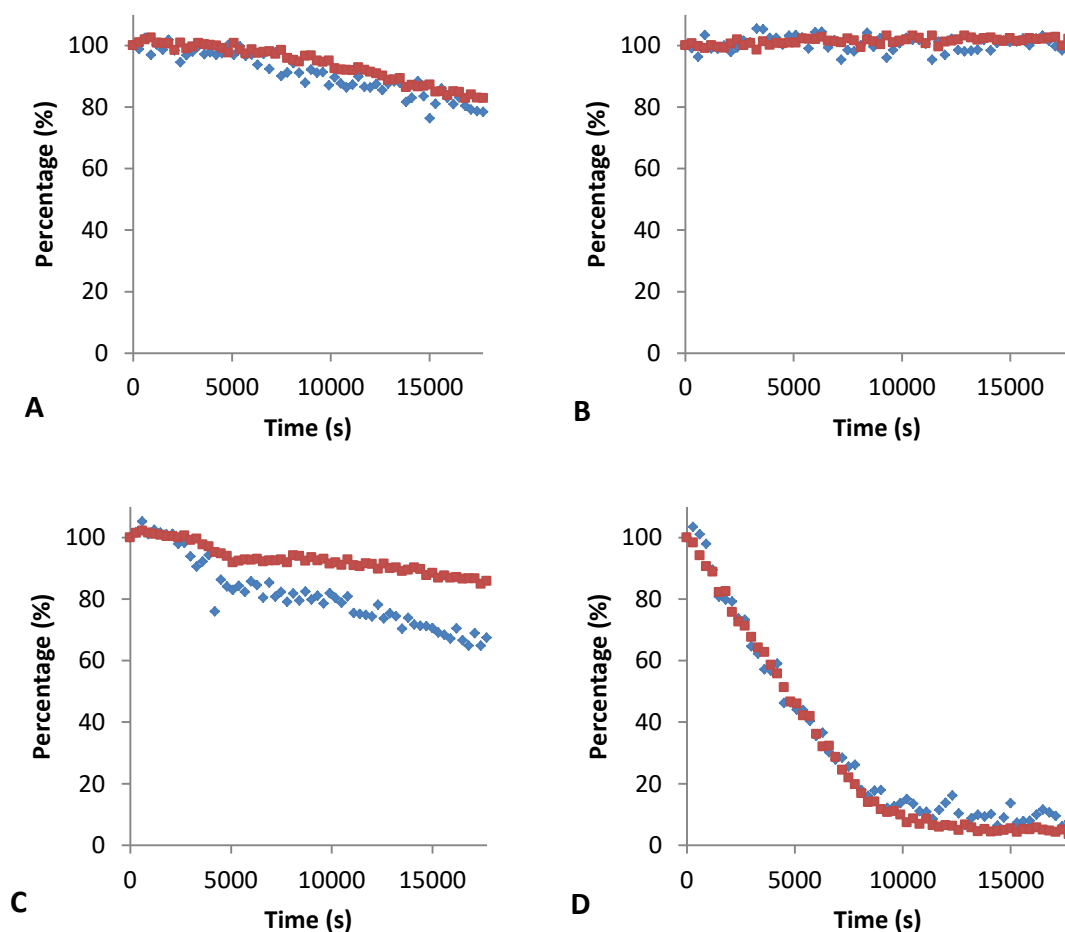


Figure 11 Time dependence of conversion of H_2O_2 (0.5 M blue diamonds) and styrene sulfonate (0.1 M, red squares) with 1 (0.1 mM) and Na_2SO_4 (0.5 M, internal reference) at pH = 8.6 and (a) no buffer, (b) sodium borate (0.1 M), (b) NaOAc (0.1 M), and (b) NaHCO_3 (0.1 M).

The effect of acetate and borate in the presence of bicarbonate, on conversion of both styrene sulfonate and H_2O_2 reveals that the presence of acetate has negligible effect in comparison to the reaction with carbonate alone (Figure 12), while the presence of borate increases the lag phase's duration and reduces the reaction rate substantially (Figure 13). Notably, however, a reduction in both the concentration of carbonate and borate results in a substantial decrease in reaction rate. These data indicate that carbonate is not acting simply as a buffer in the reaction but is actively involved, e.g., as a ligand etc.

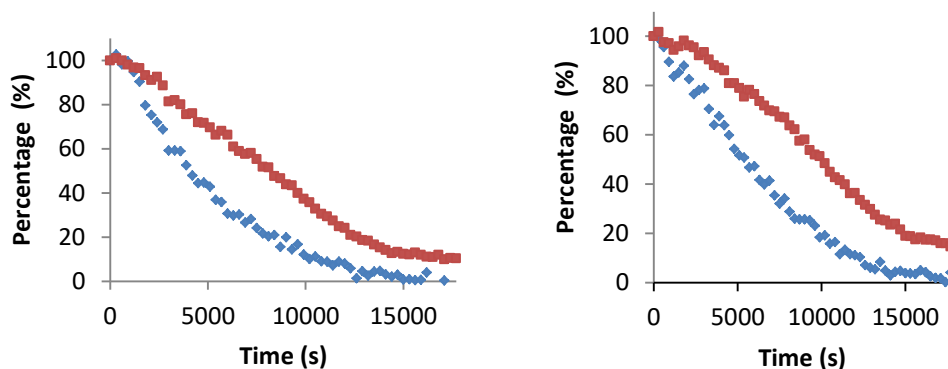


Figure 12 Time dependence of conversion of H₂O₂ (0.5 M blue diamonds) and styrene sulfonate (0.1 M, red squares) with 1 (0.1 mM) and Na₂SO₄ (0.5 M, internal reference) and NaHCO₃ (0.1 M, pH = 8.6), without (left) and with (right) NaOAc (0.1 M).

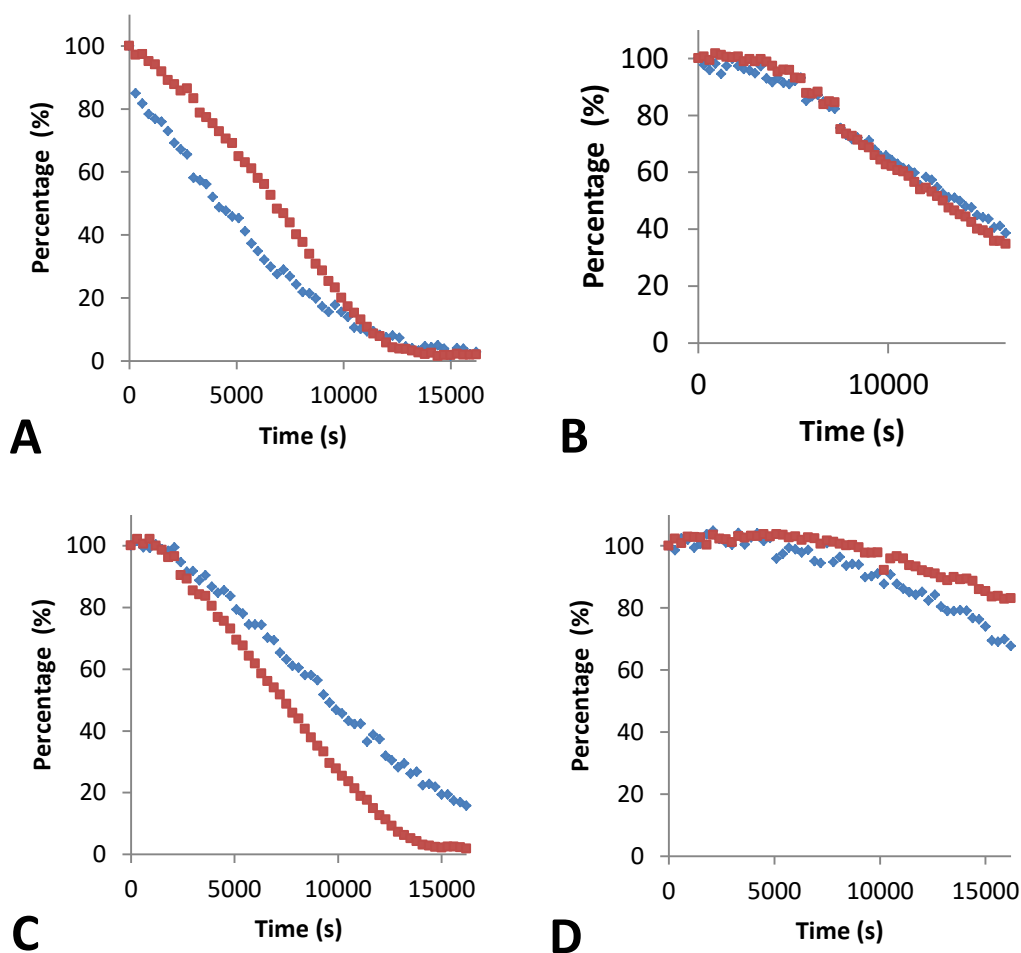


Figure 13 Time dependence of conversion of H₂O₂ (0.5 M blue diamonds) and styrene sulfonate (0.1 M, red squares) with 1 (0.1 mM) and Na₂SO₄ (0.5 M, internal reference) and NaHCO₃ (A-C 0.1 M, D 0.05 M, pH = 8.6), without (A) and with sodium borate (B 0.1 M, C & D 0.05 M).

As the borate buffer reveals a lag phase, a jump experiment was performed by adding borate (to 0.1 M) to a 0.1 M NaHCO₃(aq) solution after approx. 20% conversion of the substrate (Figure 14a). A control experiment in which 0.1 M NaHCO₃(aq) bicarbonate was added had no such effect (Figure 14b). In figure below, a drop in intensity is seen, which is observed as a drop in

concentration; however, this drop is assigned to absorption of the borate at different wavelengths.

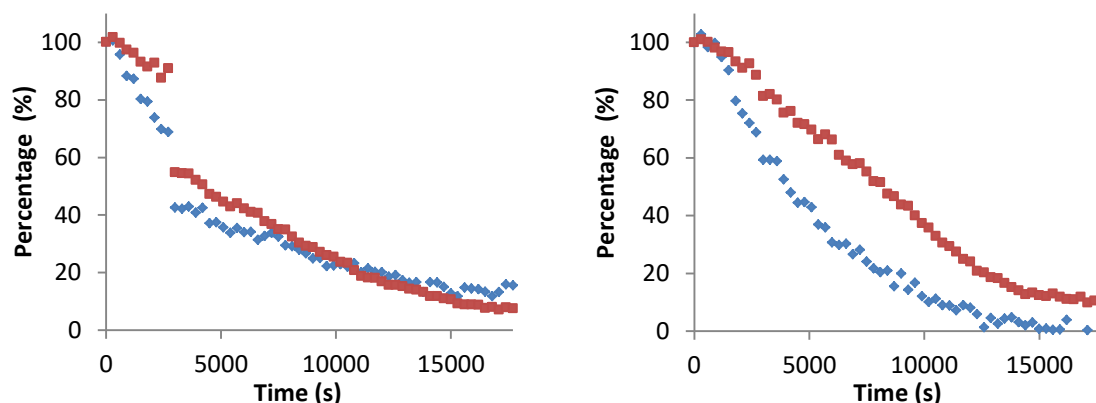


Figure 14 Time dependence of conversion of H₂O₂ (0.5 M blue diamonds) and styrene sulfonate (0.1 M, red squares) with 1 (0.1 mM) and Na₂SO₄ (0.5 M, internal reference) and NaHCO₃ (0.1 M), (left) borate (0.1 M) was added after 2700 s and (right) the same volume of buffer containing 0.1 M NaHCO₃ was added after 2700 s.

In situ formation of percarbonate.

The formation of percarbonate has been proposed by several groups to rationalise the activity of Mn(II) salts in the epoxidation of alkenes and in the bleaching of model dyes.^[17,18,10] A similar reaction could be expected in the case of borate buffer (i.e. the formation of perborate). The presence of such species under catalytic conditions was explored in an effort to understand the role of the buffering agents in catalytic oxidation of styrene sulfonate. The formation of perborate in solution is plausible, however, it is relatively insoluble in basic water and hence the effect of such a reaction would be to inhibit oxidation by removal of oxidant from the solution (vide supra).

It is conceivable that peroxido-compounds form from the reaction of H₂O₂ with CO₂, HCO₃⁻, CO₃²⁻. Raman spectroscopy 532 nm and 785 nm, however, does not provide evidence for the formation of percarbonate in solution. Comparison of the Raman spectra of a solution of commercial sodium percarbonate and of sodium bicarbonate with H₂O₂ (pH 8.5, Figure 15) reveals that the only difference between the solutions is in regard to the bands at 984 and 1070 cm⁻¹, which are due to differences in pH and hence the concentration of CO₃²⁻ and HCO₃⁻. However, the band at 984 cm⁻¹ does not correspond to any of the bands in the spectra of bicarbonate solution collected at pH between 12 and 7 (Figure 16).

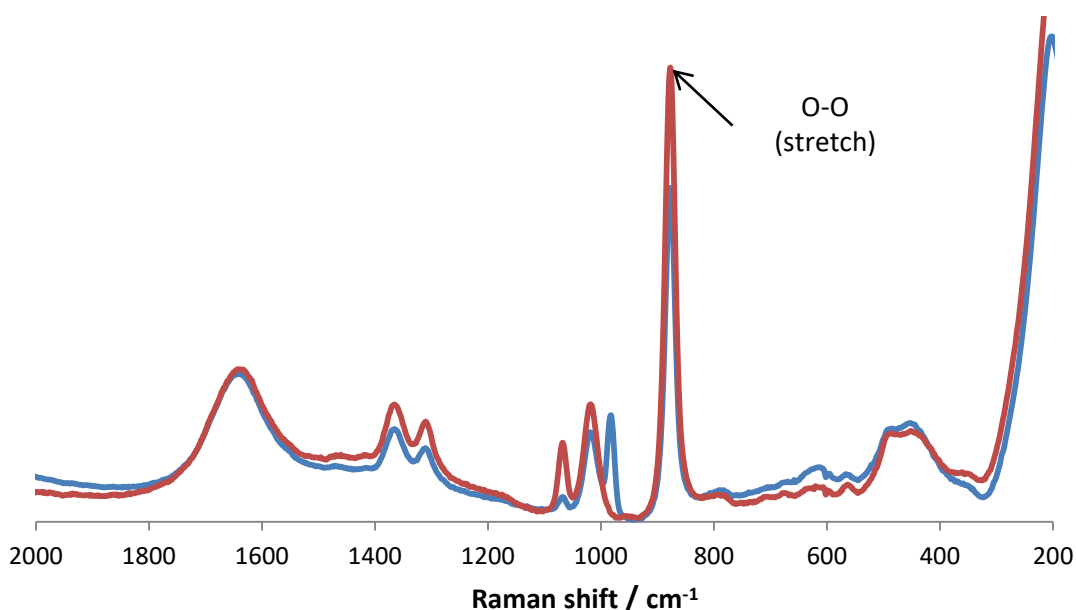


Figure 15 Comparison of Raman (λ_{exc} 532 nm) spectra of a 500 mM solution (pH 8.3) of sodium percarbonate (blue line) and of a solution of sodium bicarbonate (500 mM) and H_2O_2 (600 mM) (pH 8.7, red line).

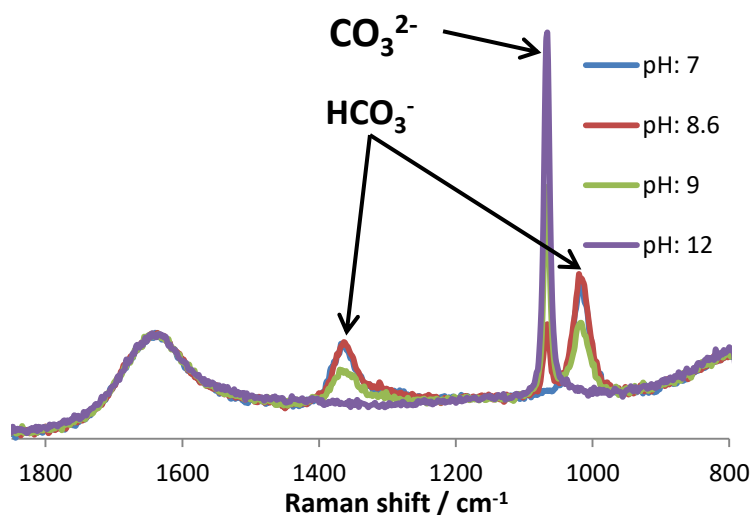


Figure 16 pH dependence of Raman (λ_{exc} 785 nm) spectrum of a NaHCO_3 (0.5 M) aqueous solution.

Catalytic activity of **1** under industrially relevant conditions:

Reaction progress monitoring of oxidation of the styrene sulfonate (SS) with H_2O_2 and **1** or Mn(II) was studied between pH 6 – 9 with a concentration of bicarbonate that is much less (10 mM) compared to studies described above and of more relevance to industrial conditions. In presence of Mn(II) , conversion of styrene sulfonate was not observed over the pH range examined.

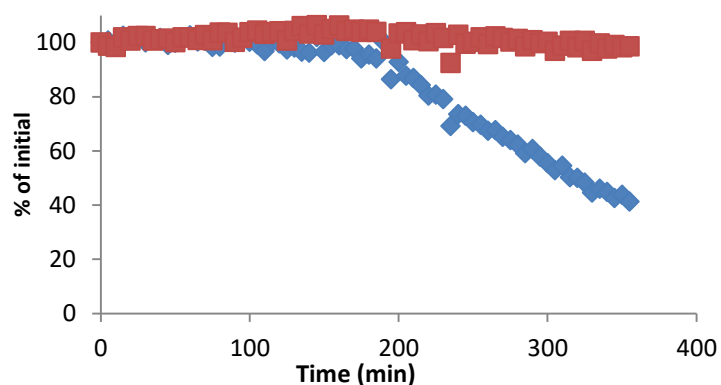


Figure 17 Time dependence of conversion of H_2O_2 (0.5 M blue diamonds) and styrene sulfonate (0.1 M, red squares) with Mn(II)SO_4 (0.2 mM) and Na_2SO_4 (0.5 M, internal reference) and NaHCO_3 (0.01 M, pH 8).

In contrast to **1**, although the reaction proceeds more slowly, conversion is observed. At pH 9 the lag phase decreases. Notably, although the rate of oxidation of styrene sulfonate shows little, if any, pH dependence, the rate of disproportionation of H_2O_2 increases with pH. (Figure 18)

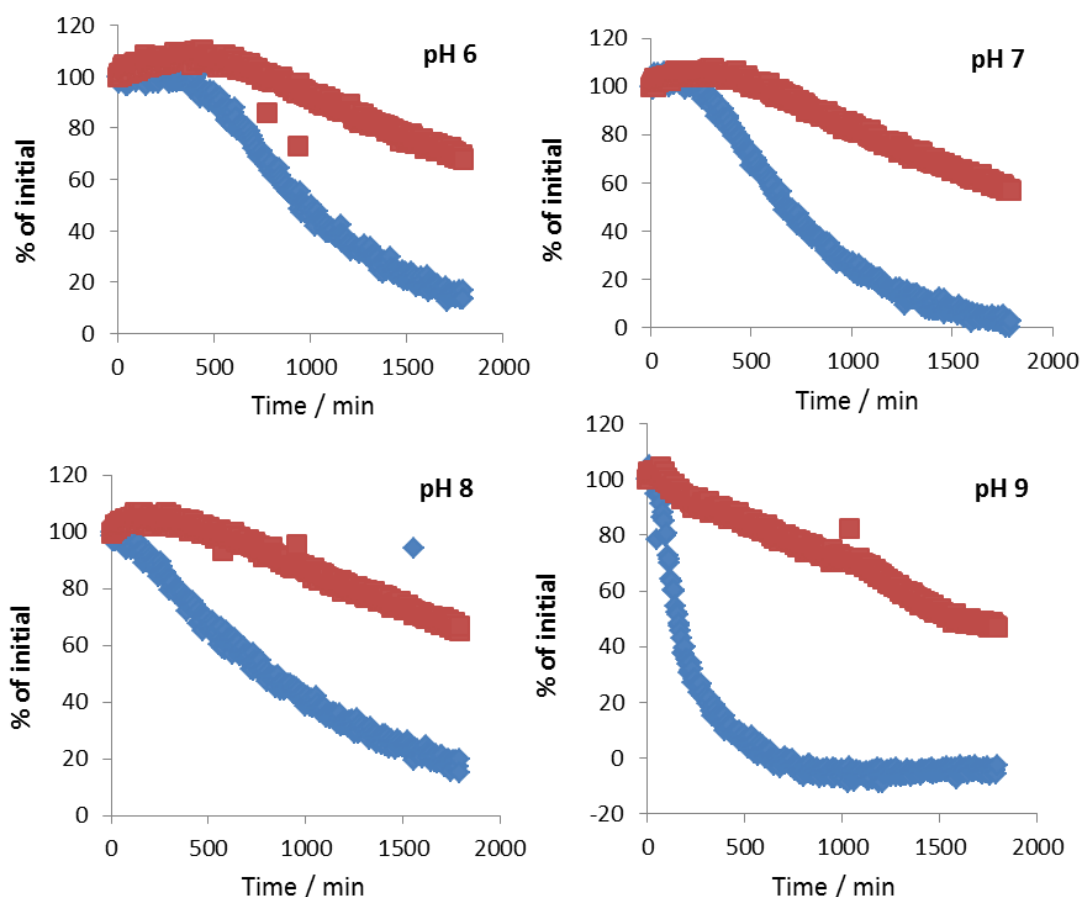


Figure 18 Time dependence of conversion of H_2O_2 (0.5 M blue diamonds) and styrene sulfonate (0.1 M, red squares) with **1** (0.1 mM) and Na_2SO_4 (0.5 M, internal reference) and NaHCO_3 (0.01 M). Upper left – pH 6, Upper right - pH 7; Lower left - pH 8; Lower right - pH 9.

5.3 Discussion

A key observation as to the physical changes that occur during the reactions is that the appearance of a brown precipitate is noticeably faster with Mn(II)SO_4 in the absence of substrate. This indicates that the formation of manganese oxides, which is thermodynamically favored at the pH of the solutions, is a slow process requiring nucleation. The dependence of the reaction rate on $\log_{10}[\text{Mn(II)}]$ is consistent with the metastable situation that is encountered in the reaction; i.e. the manganese present should be in the form of manganese oxides but the formation of these is retarded by the presence of the substrate and accelerated due to the autocatalytic nature of their formation. Given that higher oxidation states are required to form the manganese oxides, the substrate can suppress nucleation by keeping the concentration of these species low. It is not inconceivable that the concentration of carbonate has a substantial influence on these processes given the low solubility of Mn(II)CO_3 ($K_{\text{sp}} 2.24 \times 10^{-11}$). Hence, the actual steady state concentration of Mn(II) under reaction conditions is likely to be much lower than the analytical concentration. The effect of carbonate, although it is attractive to ascribe it to the formation of percarbonates, is therefore most likely due to its control on the steady state concentration of Mn(II) . At lower concentrations of carbonate, its ability to inhibit the formation of manganese oxides is reduced non-linearly. Hence, the availability of catalytically active Mn(II) ions is drastically reduced and the disproportionation of H_2O_2 by the oxides at high pH is observed.

If it is presumed that Mn(II) ions are responsible for the catalysis observed and accepted that they are only present at low concentrations, then it is possible that the primary involvement of **1** in the reaction is to provide for a slow 'leach' of Mn(II) ions into solution.

A further argument in favor of the active catalytic species at high carbonate concentrations as being Mn(II) ions is provided by the effect of DTPA. DTPA sequesters metal ions effectively and suppresses the activity of Mn(II)SO_4 completely. In the case of **1**, DTPA does not halt conversion indefinitely, however reaction monitoring by UV/Vis absorption spectroscopy indicates that after a lag time the DTPA (which contains oxidizable amines) undergoes oxidative degradation, thereby releasing and Mn(II) ions captured.

At lower concentrations, where the activity of Mn(II) ions is negligible, then the conversion of substrate can be attributed to species derived from **1**. The lower reaction rates observed indicate that it may well show the same activity at higher carbonate concentrations but this would be masked by the activity of the Mn(II) ion based catalyst.

5.4 Conclusions

The reactivity of Mn(II) and **1** towards the oxidation of alkenes in aqueous solution is similar but not identical. Mn(II) presents a greater dependence on its own concentration and that of bicarbonate as well, whereas **1** shows a linear dependence of concentration on activity and depends less strongly on the presence of bicarbonate. It is remarkable that, in contrast oxidation in acetonitrile, in water **1** is unaffected by the presence of H_2O_2 (in absence of substrate at least). The difference in the requirement for carbonate/bicarbonate in solution points towards the possible formation of percarbonate species in the case of Mn(II) catalysed reactions, however, definitive evidence for its formation is elusive. The presence of borate, inhibits catalysis and

implies the in situ formation of the oxidant sodium perborate, however, while this species has not been observed it is clear that borate removes H_2O_2 by precipitation.

The most striking, and in many ways problematic, experiment is that with DTPA, which highlights how the presence of the sequestrant can prevent oxidation with Mn(II) but does not appear to affect the activity of **1** substantially. However, it is clear from the time dependent spectroscopy that in fact DTPA undergoes oxidation and therefore releases the bound ions into solution. These data raise the question whether or not **1** is acting as a Mn(II) reservoir and provides for a jumping off point for further studies of this complex system.

5.5 Experimental

Materials

Styrene sulfonate (Sigma Aldrich) and H_2O_2 50 % aqueous solution (Acros) and all the other commercially available chemicals were used without further purification unless stated otherwise. $[\text{Mn(IV,IV)}_2(\mu\text{-O})_3(\text{tmtacn})_2](\text{PF}_6)_2$ (**1**) was available from earlier studies.^[9]

Instrumentation

Raman spectra were recorded using a Perkin-Elmer Raman Flex equipped with a fibre-optic probe (λ_{exc} 785 nm) at room temperature, typically with 10 exposures of 8 s duration. Raman spectra (λ_{exc} 355 nm) were recorded as described in chapter 4. UV/vis absorption spectra were recorded with a HP8453 spectrophotometer or a Specord600 (AnalytikJena) in 1 cm path length quartz cuvettes.

Catalysed oxidations

Oxidation of styrene sulfonate was carried out in a cuvette (3 mL total volume) according to the following protocol: Double distilled water was used to prepare a stock solution of 0.5 M Na_2SO_4 , from which a buffer solution (typically 0.1 M) was prepared. A stock solution containing the **1** or MnSO_4 (3 and 6 mM, respectively) was prepared in parallel. The reaction mixture was prepared directly in the cuvette by addition of the appropriate volumes of buffer, the catalyst and, at the start of the experiment, aq. H_2O_2 with vigorous mixing. Typical concentrations employed were 0.1 M substrate, 0.1 mM catalyst and 0.5 M H_2O_2 . Time zero is taken to be the point at which the catalyst is added. The epoxide, product of SS, was isolated and characterized by ^1H NMR spectroscopy as described elsewhere.^[13]

Analysis of Raman spectra

Raman spectra were analysed in the spectral range 1800 to 600 cm^{-1} . The data analysis used the area of the bands between 1600 and 1650 cm^{-1} , which includes contributions from the reactant and products only. The band at 870 cm^{-1} was used to determine H_2O_2 concentrations. **1** and **2** were monitored at λ_{exc} 355 nm in the range 400 to 1000 cm^{-1} .

5.6 References

-
- [1] a) J. A. Malona, K. Cariou, W. T. Spencer III, A. J. Frontier, *J. Org. Chem.*, **2012**, 77, 1891. b) M. Marigo, J. Franzén, T. B. Poulsen, W. Zhuang, K. A. Jørgensen, *J. Am. Chem. Soc.* **2005**, 127, 6964.
 - [2] a) S. S. Stahl, P. L. Alsters, "Liquid Phase Aerobic Oxidation Catalysis Industrial Applications and Academic Perspectives", Wiley-VCH, Weinheim, Germany, **2016**. b) J. R. Lokemeyer, M. Matusz, R. C. Yeates, "Epoxidation Catalyst, a Process for Preparing the Catalyst, and a Process for the Production of an Olefin Oxide", **2015**. c) R. Postma, P. Muppa, "Process for the manufacture of a 1,2-epoxide", **2014**.
 - [3] a) J.-E. Bäckvall, "Modern oxidation methods", Wiley-VCH, Weinheim, Germany, **2010**. b) J. Ichihara, A. Kambara, K. Iteya, E. Sugimoto, T. Shinkawa, A. Takaoka, S. Yamaguchi, Y. Sasaki, *Green Chemistry*, **2003**, 5, 491. c) T. Katsuki, *Chem. Soc. Rev.*, **2004**, 33, 437.
 - [4] a) K. Wieghardt, U. Bossek, B. Nuber, J. Weiss, J. Bonvoisin, M. Corbella, S. E. Vitols, J. J. Girerd, *J. Am. Chem. Soc.*, **1988**, 110, 7398. b) V. C. Quee-Smith, L. DelPizzo, S. H. Jureller, R. Hage, J. L. Kerschner, *Inorg. Chem.* **1996**, 35, 6461.
 - [5] P. Saisaha, J. W. de Boer, W. R. Browne, *Chem. Soc. Rev.*, **2013**, 42, 2059.
 - [6] K. F. Sibbons, K. Shastria, M. Watkinson, *Dalton Trans.*, **2006**, 5, 645.
 - [7] a) J. W. de Boer, W. R. Browne, J. Brinksma, P. L. Alsters, R. Hage, B. L. Feringa, *Inorg. Chem.* **2007**, 46, 6353. b) S. Abdolazadeh, J. W. de Boer, W. R. Browne, *Eur. J. Inorg. Chem.* **2015**, 3432.
 - [8] J. W. de Boer, W. R. Browne, J. Brinksma, P. L. Alsters, R. Hage, B. L. Feringa, *Inorg. Chem.*, **2007**, 46, 6353–6372
 - [9] D. Angelone, S. Abdolazadeh, J. W. de Boer, W. R. Browne, *Eur. J. Inorg. Chem.*, **2015**, 21, 3532.
 - [10] E. Ember, S. Rothbart, R. Puchta, R. van Eldik, *New J. Chem.*, **2009**, 33, 34.
 - [11] E. Ember, H. A. Gazzaz, S. Rothbart, R. Puchta, R. van Eldik, *Applied Catalysis B: Environmental*, **2010**, 95, 179.
 - [12] E. V. Bakhmutova-Albert, H. Yao, D. E. Denevan, D. E. Richardson, *Inorg. Chem.*, **2010**, 49, 11287.
 - [13] S. Abdolazadeh, N. M. Boyle, A. Draksharapu, A. C. Dennis, R. Hage, J. W. de Boer, W. R. Browne, *Analyst*, **2013**, 138, 3163.
 - [14] R. Hage, B. Krijnen, J. B. Warnaar, F. Hartl, D. J. Stufkens, T. L. Snoeck, *Inorg. Chem.*, **1995**, 34, 4973.
 - [15] S.-H. Shim, D. LaBounty, T. S. Duffy, *Phys. Chem. Minerals*, **2011**, 38, 685.
 - [16] C. Julien, M. Massot, S. Rangan, M. Lemal, D. Guyomard, *J. Raman Spectrosc.* **2002**, 33, 223.
 - [17] B. S. Lane, M. Vogt, V. J. DeRose, K. Burgess, *J. Am. Chem. Soc.*, **2002**, 124, 40, 11946.
 - [18] D. E. Richardson, H. Yao, K. M. Frank, D. A. Bennett, *J. Am. Chem. Soc.* **2000**, 122, 1729.